Effects of Equal Angle Resampling on Pointing and Cloud Displacement Measurement Accuracy

L. A. Sromovsky

15 August 1972

University of Wisconsin
Space Science and Engineering Center
1225 West Dayton Street
Madison, Wisconsin

Forward

Equal Angle (EA) resampling of S/C Equal Time (ET) samples introduces a relatively small RMS time jitter of approximately 0.3 μsec, resulting in an RMS position error of approximately 0.06 n. mi. at the subsatellite point. However, this error is not random along a scan line but, instead, displays a periodic variation that can lead to false indications E-W convergence and wind shear.

A major portion of this document is devoted to the precise mathematical description of the error patterns produced by the EA resampling, thus providing a basis for computer simulation and analysis. A hand calculation of a sixteen line error field is included as an example of errors that can result in the measured displacements of small clouds that move parallel to scan lines. This example represents a worst case situation. Large clouds and clouds with variable N-S motions would not show such distinctive error patterns because of their inherent error averaging characteristics.

Preliminary results presented here indicate that EA resampling will not be a major problem in cloud displacement measurements. In practical situations (which need some kind of specification) it is quite probable that the variety of cloud sizes and motions will reduce the resampling error to the equivalent of a random uncorrelated error of 0.3 μsec RMS. This conjecture can be tested by computer simulation if necessary. If this conjecture is found to be erroneous, a suggested method can be employed to reduce the resampling error to acceptable levels.

TABLE OF CONTENTS

I. SYSTEM OPERATION (Figure 1):

1) S/C Video Sampling and Transmission

1.1) Time between samples = τ_{ET}, determined by S/C 14 MHz bit rate clock divided down to 500 kHz, independent of spin rate.

1.2) Start of video sampling determined by Earth Angles Generator and ultimately by the S/C Spin Clock which has a resolution of 0.2° and an absolute angular accuracy of 0.5°.

2) CDA Interpolation

2.1) At CDA interpolated samples are inserted midway between original S/C samples.

2.2) The interpolated samples are formed from linear combinations of the adjacent two (or adjacent four) original samples.

2.3) The time spacing between adjacent members of this augmented set of samples is $\frac{1}{2}\tau_{ET}$.

3) CDA Equal Angle Resampling

3.1) The timing of EA resampling is controlled by the CDA PLL (Phase Locked Loop) which is locked to the smoothed S/C spin rate.

3.2) The nominal time between adjacent equal angle samples = τ_{EA}, obtained by dividing the S/C spin period into a fixed number of angular increments, and thus depending on spin rate.

3.3) The start of EA (Equal Angle) resampling is determined by the sun synch pulse output of the CDA PLL shifted by the Earth Sun angle. Timing accuracy at 100 RPM is approximately 0.30 μ sec (≃ 3 μ radians).

3.4) Whenever the EA clock calls for an EA sample, the actual sample selected is the augmented set sample which occurs nearest in time to the EA request.

3.5) The selected samples are subsequently treated as equal angle samples although their actual time locations can differ from the nominal EA time by as much as $\frac{1}{4}\tau_{ET}$. This leads to a systematic timing (or, equivalently, positional) error in the EA samples.

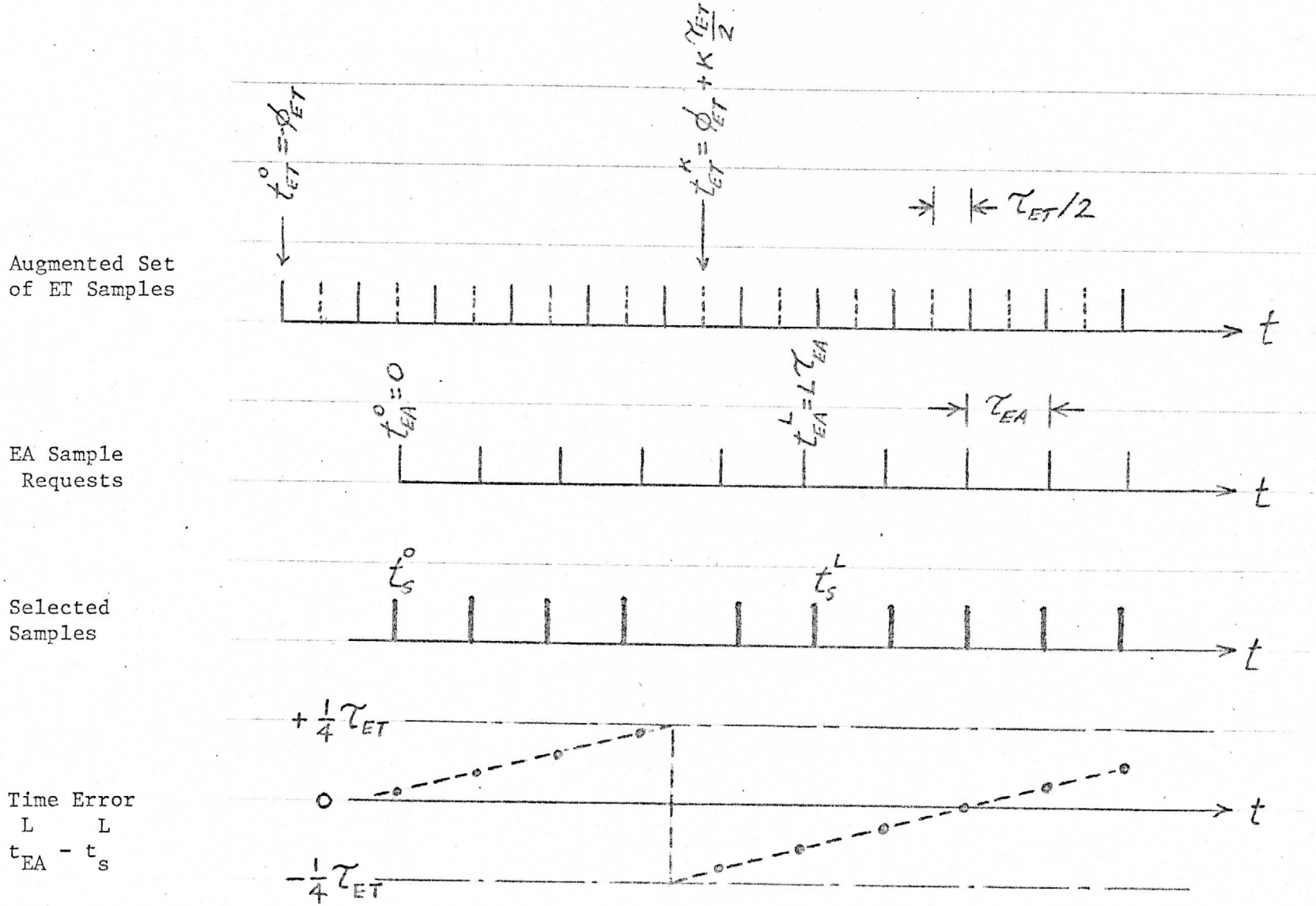

Figure 1. Resampling System Operation

II. DERIVATION OF EA TIMING ERROR:

1) Definitions:

τ_{ET} = time between S/C ET samples

$\frac{1}{2}\tau_{ET}$ = time between AUGMENTED ET samples

τ_{EA} = time between EA sample requests

t_{ET}^{K} = the time location of the kth sample of the augmented ET set

t_{EA}^{L} = the time at which the Lth EA sample is requested

t_{s}^{L} = the time location of the sample selected as the Lth EA sample

ϕ_{ET} = $t_{EA}^{o} - t_{ET}^{o}$, the time interval between the EA start time and the ET start time

INT(X) = the largest integer $\leq$ X

2) Derivation:

Assuming that $t_{EA}^{o} = 0$, we can write

$$t_{ET}^{K} = K \frac{1}{2}\tau_{ET} - \phi_{ET} \qquad (1)$$

$$t_{EA}^{L} = L\tau_{EA} \; . \qquad (2)$$

The ET sample chosen as the Lth EA sample is determined by

$$-1/4\tau_{ET} < t_{EA}^{L} - t_{ET}^{K_L} \leq \frac{1}{4}\tau_{ET}. \qquad (3)$$

Substituting (1) and (2) in (3) yields

$$-\frac{1}{2}\tau_{ET} < L\tau_{EA} - K_L\frac{1}{2}\tau_{ET} + \phi_{ET} \leq \frac{1}{4}\tau_{ET}, \tag{4}$$

which reduces to the set of conditions

$$X_L - 1 \leq K_L < X_L, \quad \text{where} \tag{5}$$

$$X_L = 1/2 + \frac{2}{\tau_{ET}}(L\tau_{EA} + \phi_{ET}). \tag{6}$$

The only solution is given by

$$K_L = \text{INT}(X_L) = \text{INT}(1/2 + \frac{2}{\tau_{ET}}(L\tau_{EA} + \phi_{ET})). \tag{7}$$

The actual time of the sample selected as the Lth EA sample is thus

$$t_S^L = t_{ET}^{K_L} = \frac{1}{2}\tau_{ET}\text{INT}(1/2 + \frac{2}{\tau_{ET}}(L\tau_{EA} + \phi_{ET})) - \phi_{ET} \tag{8}$$

and the time error of the Lth EA sample is

$$t_{EA}^L - t_S^L = L\tau_{EA} + \phi_{ET} - \frac{1}{2}\tau_{ET}\text{INT}(1/2 + \frac{2}{\tau_{ET}}(L\tau_{EA} + \phi_{ET})). \tag{9}$$

Equation (9) expresses the time error as a difference of two rapidly varying functions of L. By cancelling off the rapidly varying components of each term the actual error dependence can be made more transparent. Since

$$\text{INT}(A + I) = I + \text{INT}(A), \forall A \text{ if } I = \text{integer},$$

equation (9) can be rewritten as

$$t_{EA}^L - t_S^L = \frac{1}{2}\tau_{ET}[A_L - \text{INT}(A_L + 1/2)], \tag{11}$$

where,

$$A_L = 2L(\frac{\tau_{EA}}{\tau_{ET}} - 1) + 2\frac{\phi_{ET}}{\tau_{ET}}. \tag{12}$$

Note that the initial EA timing error is

$$e_o = t_{EA}^o - t_S^o = \phi_{ET} - \frac{1}{2}\tau_{ET}\text{INT}(2\frac{\phi_{ET}}{\tau_{ET}} + 1/2). \tag{13}$$

The L-dependence of the error is shown in Figure 2 for $\tau_{EA} > \tau_{ET}$ and $\frac{\tau_{EA}}{\tau_{ET}} - 1 << 1$. For $\tau_{EA} < \tau_{ET}$ it would show a linear decrease between jumps rather than an increase. If $\frac{\tau_{EA}}{\tau_{ET}}$ were not close to unity the time interval (and L interval) between jumps would decrease. The $\frac{1}{2}\tau_{ET}$ jumps in EA time error occur whenever A_L crosses a half integer value. Since the slope of A_L is

$$\frac{dA_L}{dL} = 2\left[\frac{\tau_{EA}}{\tau_{ET}} - 1\right], \tag{14}$$

the mean L-spacing between EA error jumps is given by

$$\Delta L = \left| \frac{1}{2\left[\frac{\tau_{EA}}{\tau_{ET}} - 1\right]} \right| . \tag{15}$$

3) Notes on timing error period (Figure 3)

(3.1) The EA angular increments are such that $\tau_{EA} = \tau_{ET}$ for a spin rate of 100.16 RPM

(3.2) The nominal S/C spin rate is 100 ±1 RPM

(3.3) In terms of spin rate w equation (16) can be written as

$$\Delta L = \frac{w}{2|w_o - w|} , \tag{17}$$

where w_o = 100.16 RPM.

4) Notes on initial timing error

(4.1) The initial timing error can be written as

$$e_o = \frac{1}{2}\tau_{ET}\left[2\frac{\phi_{ET}}{\tau_{ET}} - \mathrm{INT}\left(2\frac{\phi_{ET}}{\tau_{ET}} + 1/2\right)\right], \tag{18}$$

where ϕ_{ET} is the time interval between ET and EA start times.

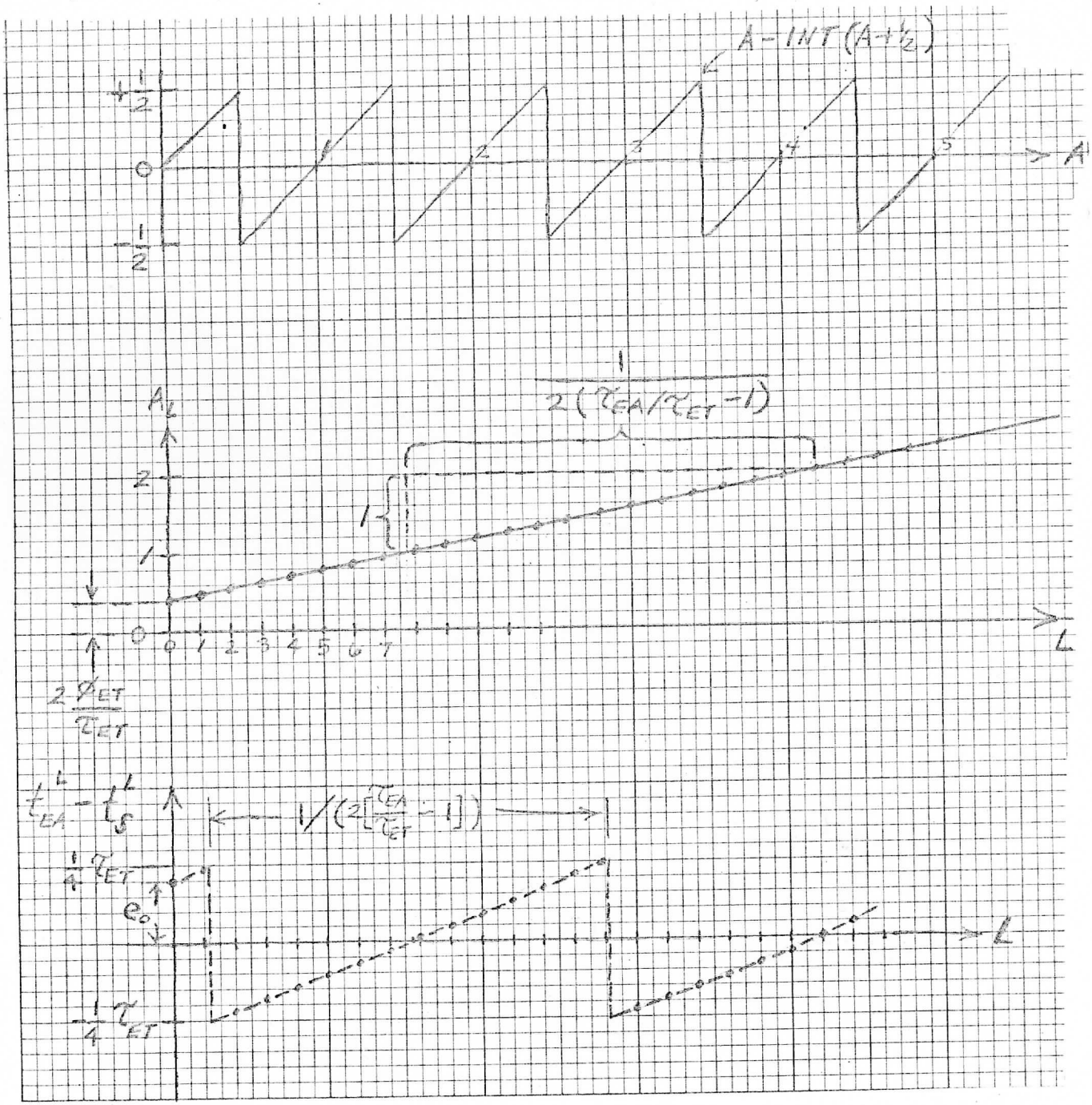

Figure 2. EA Timing Error

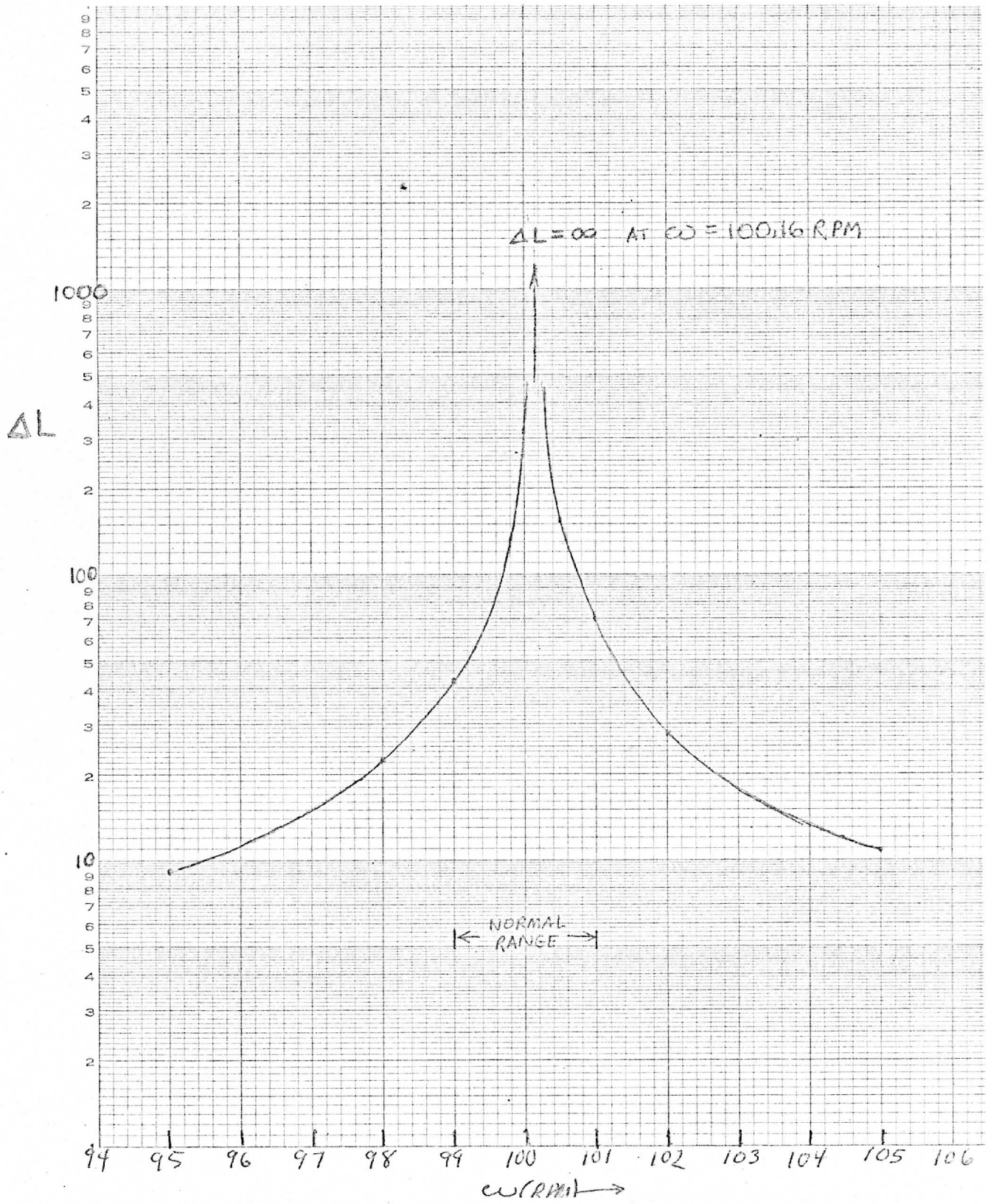

Figure 3. Timing error period as a function of spin rate.

4.2) Since the ET start time is determined by a S/C timing system which has an angular resolution of only about 0.2° of an SMS rotation, the rotation to rotation jitter of ϕ_{ET} will be large compared to τ_{ET}. Considering this fact and the form of equation (18), ϕ_{ET}/τ_{ET} may be considered as a random variable uniformly distributed over the interval (0, 1/2).

4.3) Line to line variations of ϕ_{ET}/τ_{ET} will not be random if the lines in question are scanned during the same rotation, i.e., if they belong to the same eight-line group. Since the eight VISSR visible detectors are sampled sequentially at intervals of 1.5 μsec/7 ≃ .214 μ sec between detectors, the ET to EA start times for the visible channels will satisfy

$$\phi_{ET}^{K} = \phi_{ET}^{1} - (K-1)0.214 \text{ μsec} \quad , \quad K = 1,\ldots,8, \tag{19}$$

where ϕ_{ET}^{1} is the time difference for line 1 of the eight line group and ϕ_{ET}^{K} is the time difference for the Kth line of the group. Equation (19) is useful for estimating the average pointing error for averaged data.

III. EQUATIONS FOR RESAMPLING TIMING ERROR SIMULATION

1) Simulation of ET to EA starting time difference: Defining

F = frame number

S = scan number (rotation number within frame)

RL = relative line number within the Sth scan,

the starting time difference is given by

$$\phi_{ET}(F,S,RL) = \phi_{ET}(F,S) - (RL-1)\Delta\tau, \tag{20}$$

where

$\Delta\tau$ = sequential sampling time interval (0.21 μ sec for VISSR visible channels) and, where $\phi_{ET}(F,S)$ is chosen as a random variable uniformly distributed over the interval $(0, \frac{1}{2}\tau_{ET})$.

2) Simulating the time location of each EA sample: According to equation (8), the actual time of the Lth EA sample of the Fth frame, Sth scan and RLth line within the Sth scan is

$$t_s^L(F,S,RL) = \frac{1}{2}\tau_{ET}\,\mathrm{INT}\left(1/2 + \frac{2}{\tau_{ET}}(L\tau_{EA} + \phi_{ET}(F,S,RL))\right) - \phi_{ET}(F,S,RL) \tag{21}$$

where

$\phi_{ET}(F,S,RL)$ is given by equation (20).

3) Simulation of the EA timing error: According to equation (11) the difference between the EA request time and the actual time of the selected sample is given by

$$e_L(F,S,RL) = [t_{EA}^L - t_s^L]_{F,S,RL} = \frac{1}{2}\tau_{ET}\,[A_L(F,S,RL) - \mathrm{INT}[A_L(F,S,RL) + 1/2]] \tag{22}$$

where,

$$A_L(F,S,RL) = 2L\left(\frac{\tau_{EA}}{\tau_{ET}}\right) + 2\,\frac{1}{\tau_{ET}}\,\phi_{ET}(F,S,RL), \tag{23}$$

where, as before, $\phi_{ET}(F,S,RL)$ is given by equation (20).

4) Conversion to errors in angle: If T is the satellite spin period, then the angular pointing error δ_L can be obtained from the timing error e_L according to

$$\delta_L = 2\pi\,\frac{e_L}{T}\,. \tag{24}$$

IV. DISPLACEMENT ERRORS:

1) Small Clouds (displacement error of two elements). Consider two different EA samples located at (F,S,RL,L) and (F',S',RL',L') respectively. Since no data averaging is involved it is sufficient to consider only the coordinates (F,L) and (F',L'). The inferred relative time displacement is given by

$$t_{EA}^{L',F'} - t_{EA}^{L,F} = t_S^{L',F'} - t_S^{L,F} + [e_{L'}(F') - e_L(F)] \tag{25}$$

where $t_s^{L',F'} - t_S^{L,F}$ is the actual relative time displacement of the selected samples and $[e_{L'}(F') - e_L(F)]$ is the displacement error. Making use of equation (23) the displacement error can be written as

$$[e_{L'}(F') - e_L(F)] = \frac{1}{2}\tau_{ET}[Y + INT(B) - INT(B + Y)], \tag{26}$$

where

$$Y = 2(L' - L)\left[\frac{\tau_{EA}}{\tau_{ET}} - 1\right] + \frac{2}{\tau_{ET}}[(\phi_{ET}(F'') - \phi_{ET}(F)], \tag{27}$$

$$B = 2L\left(\frac{\tau_{EA}}{\tau_{ET}} - 1\right) + \frac{2}{\tau_{ET}}\phi_{ET}(F) + 1/2.$$

For fixed Y (same L'-L difference) the displacement error [e'-e] is a square wave function of the variable B (or L). Defining

$$Y = Y_I + Y_F \quad \text{where} \quad Y_I = INT(Y), \tag{28}$$

we find

$$[e'-e] = \frac{1}{2}\tau_{ET}[Y_F + INT(B) - INT(B + Y_F)] \tag{29}$$

which satisfies the square wave conditions

$$\begin{aligned} [e'-e] &= \frac{1}{2}\tau_{ET}Y_F \quad \text{for} \quad N \leq B \leq N + 1 - Y_F \\ [e'-e] &= \frac{1}{2}\tau_{ET}(Y_F - 1) \quad \text{for} \quad N - Y_F \leq B < N. \end{aligned} \tag{30}$$

This function is displayed in Figure 4. Note that the total variation of the displacement error, i.e., $[e'-e]_{max} - [e'-e]_{min}$, is independent of Y_F and equal to $\frac{1}{2}\tau_{ET}$. Note that the L-period of the square wave cycles is given by equation (15) or (17). The L-distance corresponding to Y_F is just the product of Y_F and the L-period.

For fixed B (equivalent to fixed L), [e'-e] is a sawtooth function of the variable Y. If we define

$$B = B_F + B_I, \quad \text{where} \quad B_I = INT(B), \tag{31}$$

then the displacement error can be expressed as

$$[e'-e] = \frac{1}{2}\tau_{ET}[Y - INT(B_F + Y)]. \tag{32}$$

Since L is assumed fixed and $(\tau_{EA}/\tau_{ET} - 1)$ is assumed positive, Y is an increasing function of L' (actually L'-L). The L'-L period of the sawtooth is given by equation (15) or (17), and the total error range $[e'-e]_{max} - [e'-e]_{min}$ is independent of B_F and equal to $1/2\tau_{ET}$. The function is displayed in Figure 5. The L' (or L'-L) distance corresponding to B_F is obtained, of course, by the multiplication of B_F and the L'-L period.

2) An example of a small cloud error field

2.1) Assumed conditions: $\Delta L = 100$ (equivalent to w = 100.56 RP,); Relative Navigation of the two frames is accomplished by alignment of relative line 3 of scan 2 of frame 1 with relative line 1 of scan 1 of frame 2. (Longitude shifts need not be considered); Relative cloud displacements (measured in units of EA elements) are: small compated to ΔL (this allows Y of equation (27) to be assumed constant along a line) and parallel to scan lines (this is required to insure a unique error field); Basic time intervals are $\tau_{ET} = 2.0$ μsec and $\Delta\tau = 0.214$ μsec.

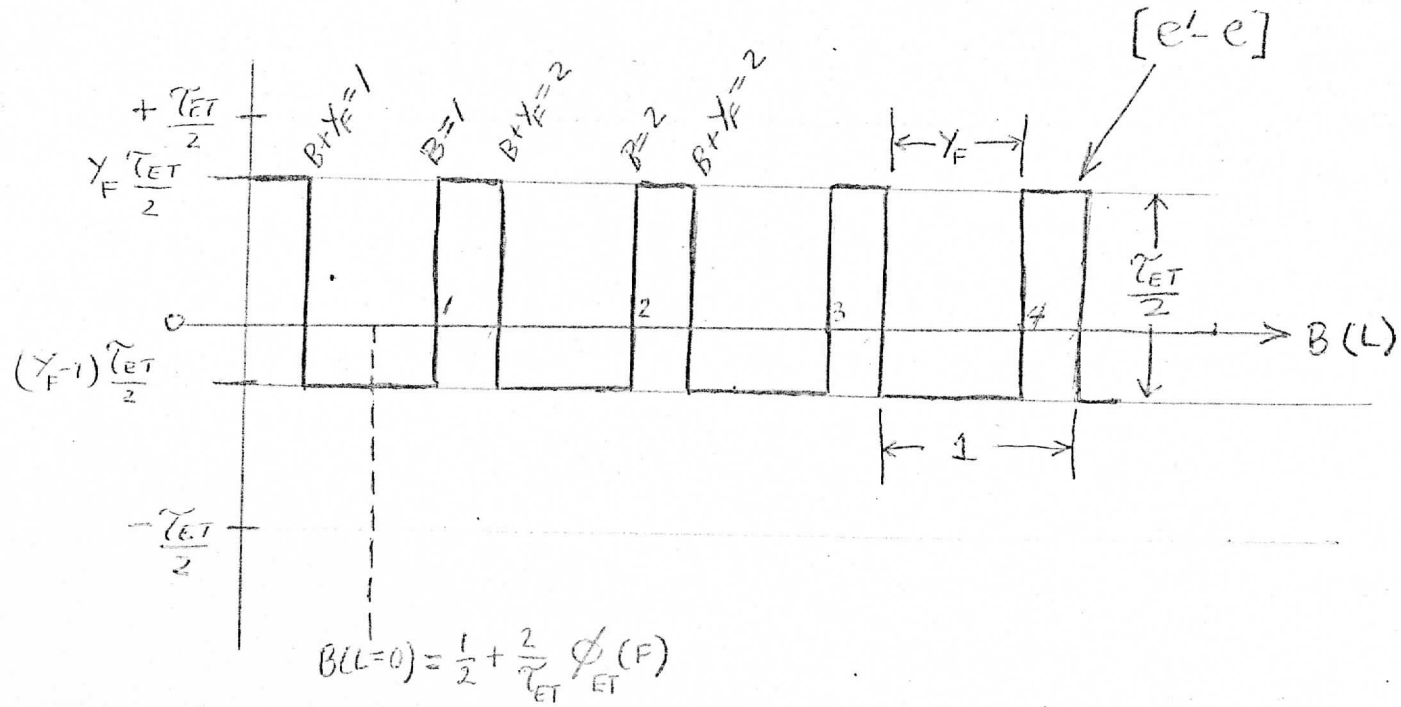

Figure 4. Displacement errors as a function of L for fixed Y.

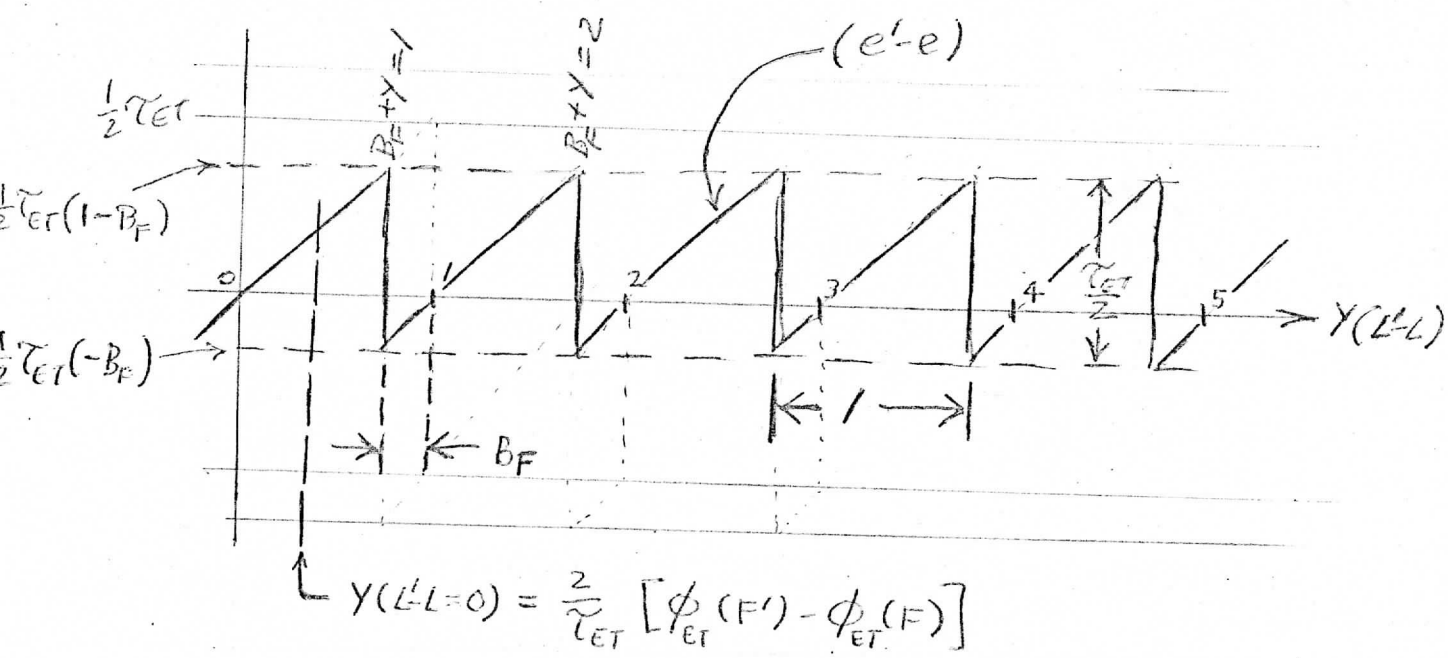

Figure 5. Displacement errors as a funciton of (L'-L) for fixed B.

2.2) Calculation Summary: The calculation of the square wave error parameters is displayed in Table 1 for a sixteen (16) line swath. For each of the four scans (rotations) a starting time is chosen at random. The remaining starting times are determined from equation (20). Given the values of Y_F it is possible to construct appropriate square wave error plots as a function of B, as shown in Figure 6.. From the B(L=0) values (indicated by arrows in Figure 6) and the fact that one unit of B corresponds to 100 units of L, the displacement error as a function of element position along a line can be found for each line. The results are displayed as an array in Figure 7. Each unit represents 0.10 μsec relative time location error, or ≃ 1μ radian, or ≃ 0.025 n. mi at the subsatellite point. The largest displacement error for this example is 8 x 0.025 n. mi. = 0.2 n. mi. For a frame interval of 30 minutes this would result in a wind error of 0.4 knots or 0.2 m/sec (at the subsatellite point). The displacements shown are the amounts by which the apparent displacements exceed the actual displacements.

The wind vector error field corresponding to Figure 7 is shown in Figure 8. Recall that all these results apply only to clouds which do not move perpendicular to scan lines. Although it is possible to calculate displacement errors for such motions, the error field can no longer be specified uniquely by line and element. A third dimension, specifying the extent of perpendicular motions, would be required. For a frame interval of 30 minutes, the largest vector corresponds to an error of 0.2 m/sec and the shortest to an error of 0.05 m/sec.

The wind error patterns of Figure 8 lead to similar patterns of horizontal convergence (parallel to the scan direction) and wind shear (perpendicular to the scan direction). These patterns are shown in Figure 9. If adjacent wind

Table 1. Sample timing error calculation.

LINE	FRAME 2 S'	FRAME 2 RL'	FRAME 2 ϕ'_{ET} μsec	FRAME 1 S	FRAME 1 RL	FRAME 1 ϕ_{ET} μsec	$\frac{\phi_{ET} - \phi_{ET}}{\tau_{ET}/2}$	Y_F	$Y_F - 1$	B(L=0)	B(L=0) - INT(B(L=0))
1	1	1	1.500	2	3	1.300	0.20	0.20	-.80	1.80	0.80
2		2	1.286		4	1.086	0.20	0.20	-.80	1.59	0.59
3		3	1.072		5	0.872	0.20	0.20	-.80	1.37	0.37
4		4	0.858		6	0.658	0.20	0.20	-.80	1.16	0.16
5		5	0.642		7	0.442	0.20	0.20	-.80	0.94	0.94
6		6	0.428		8	0.228	0.20	0.20	-.80	0.73	0.73
7		7	0.214	3	1	1.800	-1.59	0.41	-.59	2.30	0.30
8		8	0.000		2	1.586	-1.59	0.41	-.59	2.09	0.09
9	2	1	2.200		3	1.372	0.83	0.83	-.17	1.87	0.87
10		2	1.986		4	1.158	0.83	0.83	-.17	1.66	0.66
11		3	1.772		5	0.942	0.83	0.83	-.17	1.44	0.44
12		4	1.558		6	0.728	0.83	0.83	-.17	1.23	0.23
13		5	1.342		7	0.514	0.83	0.83	-.17	1.01	0.01
14		6	1.128		8	0.300	0.83	0.83	-.17	1.80	0.80
15		7	0.914	4	1	1.514	-0.60	0.40	-.60	2.01	0.01
16		8	0.700		2	1.300	-0.60	0.40	-.60	2.80	0.80

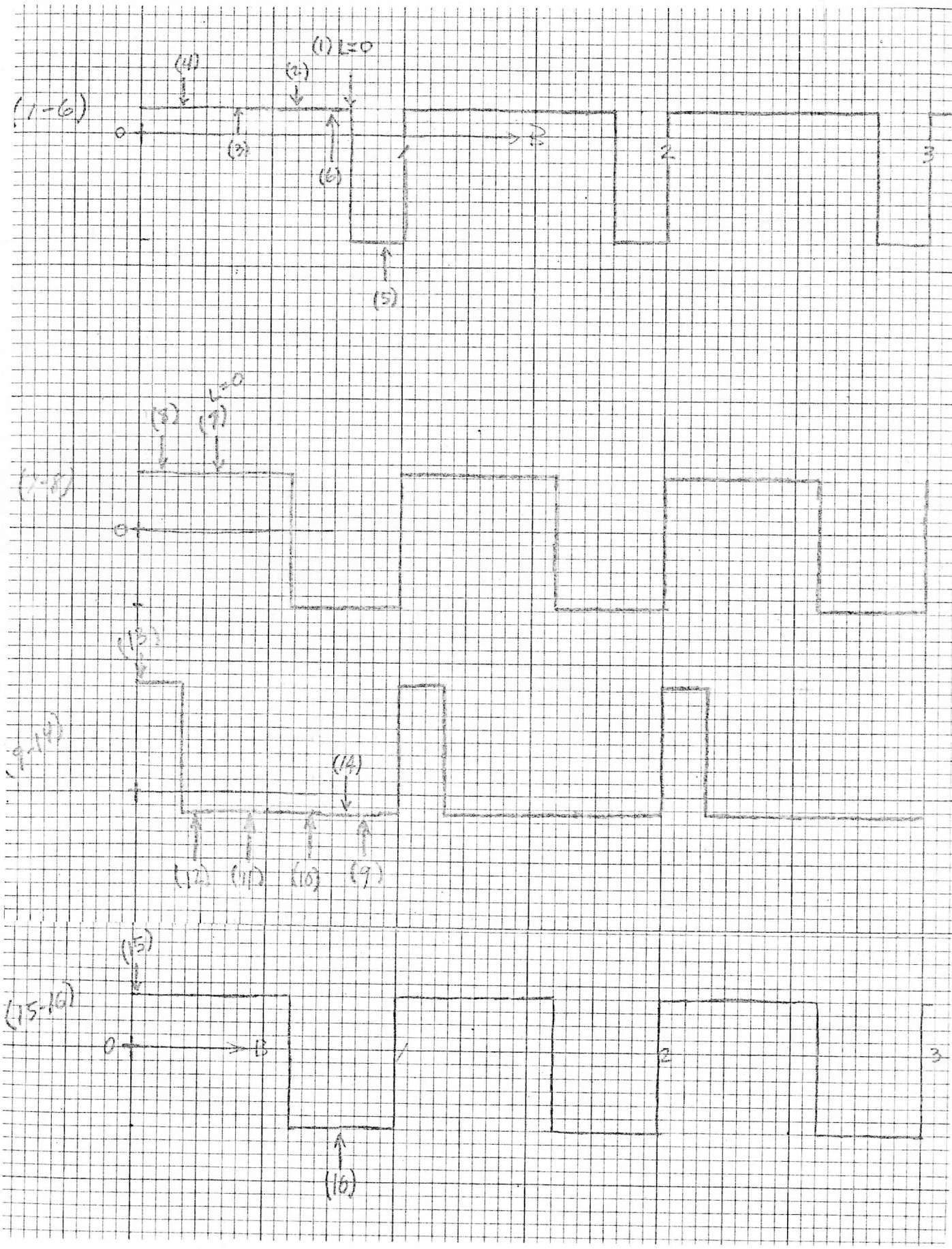

Figure 6. Error waveforms used in example calculations.

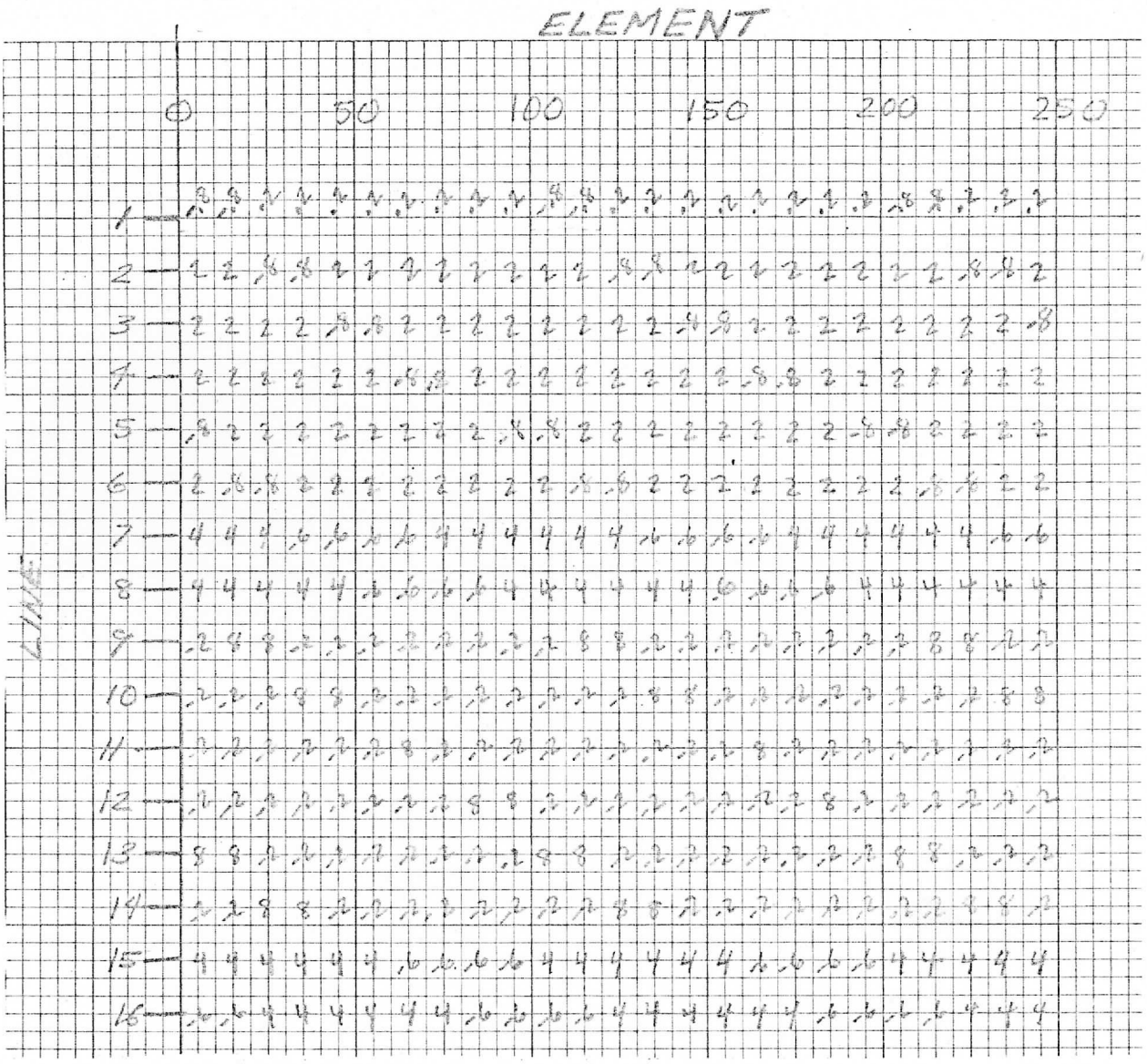

Figure 7. Displacement Error Field

1 Unit = 0.10 μsec or 1μ radian or 0.025 n. mi.

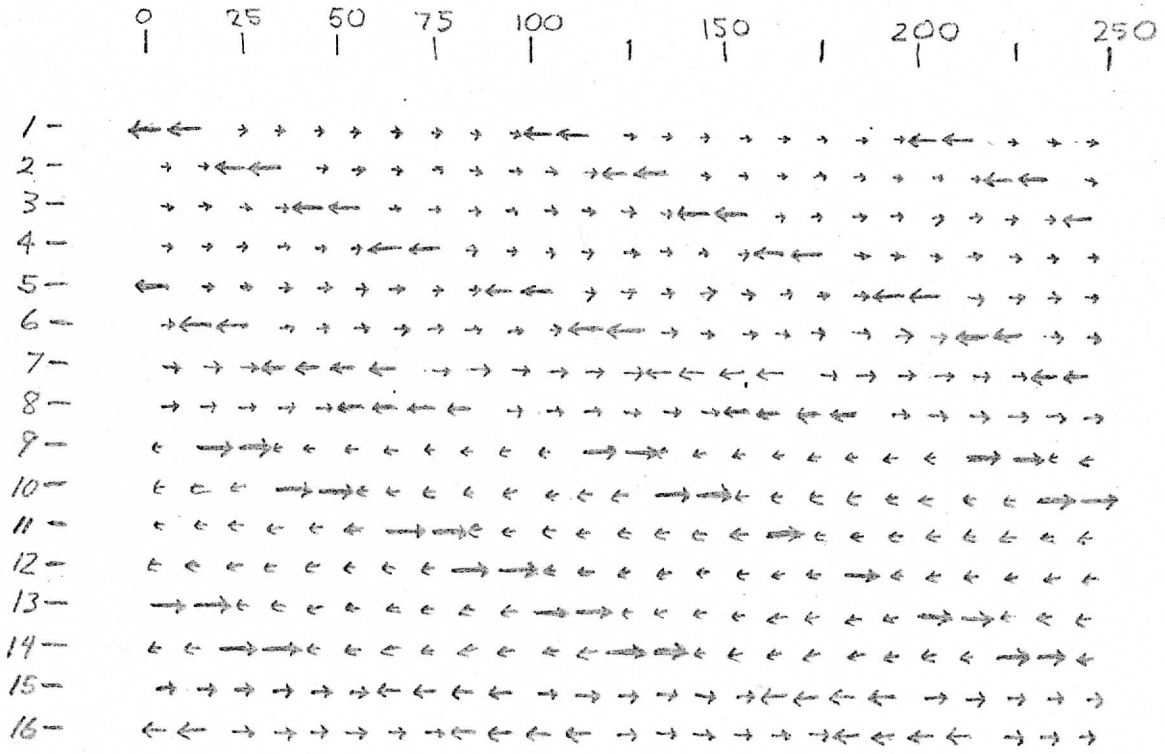

Figure 8. Wind Vector Error Field. The longest vector corresponds to a wind error of 0.2 m/sec for a 30 minute frame interva.

error vectors (along a line) are pointing toward each other the convergence is taken as positive (+). If adjacent wind error vectors on neighboring lines shown an increase (to the right) with increasing line number the shear is taken as positive (+). Typical values of convergence are near 0.5 knots (0.25 m/sec) relative velocity. The typical wind shear magnitude is near 0.5 knots/line.

3) Effects of resampling errors on large cloud displacements

Measurement of large cloud displacements is, in essence, the measurement of the mean displacement of a group of elements. As a result, considerable averaging of resampling displacement errors can occur. Although exact determination of the mean displacement error depends on the line-element locations corresponding to the cloud in question, two general characteristics of the error averaging can be stated:

(i) averaging displacements along a line is relatively ineffective in reducing displacement error unless the averaging length is $\geq \Delta L$ (the error cycle period). This is due to the slow variation of displacement error with L.

(ii) averaging displacements of elements on different lines is effective because of the random starting time for each scan (rotation) and the skewed sampling of the eight lines within each scan.

As an example of averaging characteristics, consider the average displacement error of four-line element averages. Using the single line results presented in Figure 7, the four line results are found to be those displayed in Figure 10. Note that the displacement error magnitude is considerably reduced overall compared to the individual line errors. Averaging more than four lines would show an even greater error reduction. Similar reductions appear in the convergence error and wind shear errors.

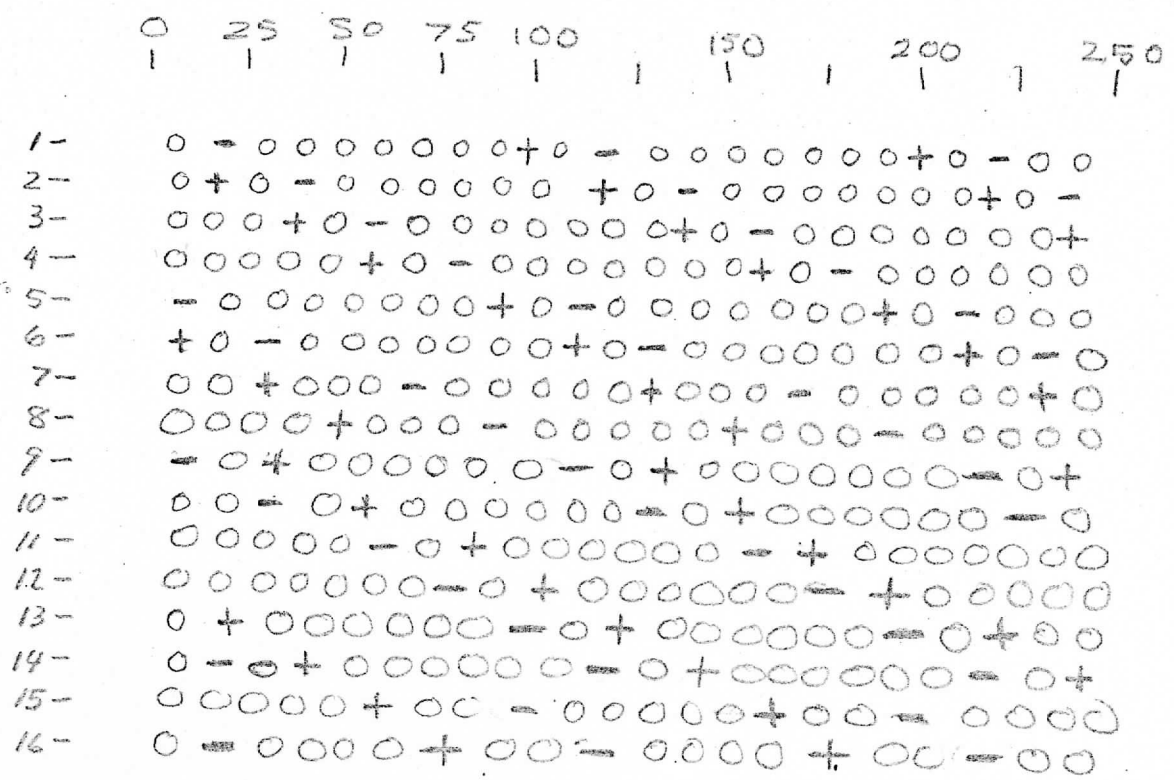

CONVERGENCE ERROR FIELD

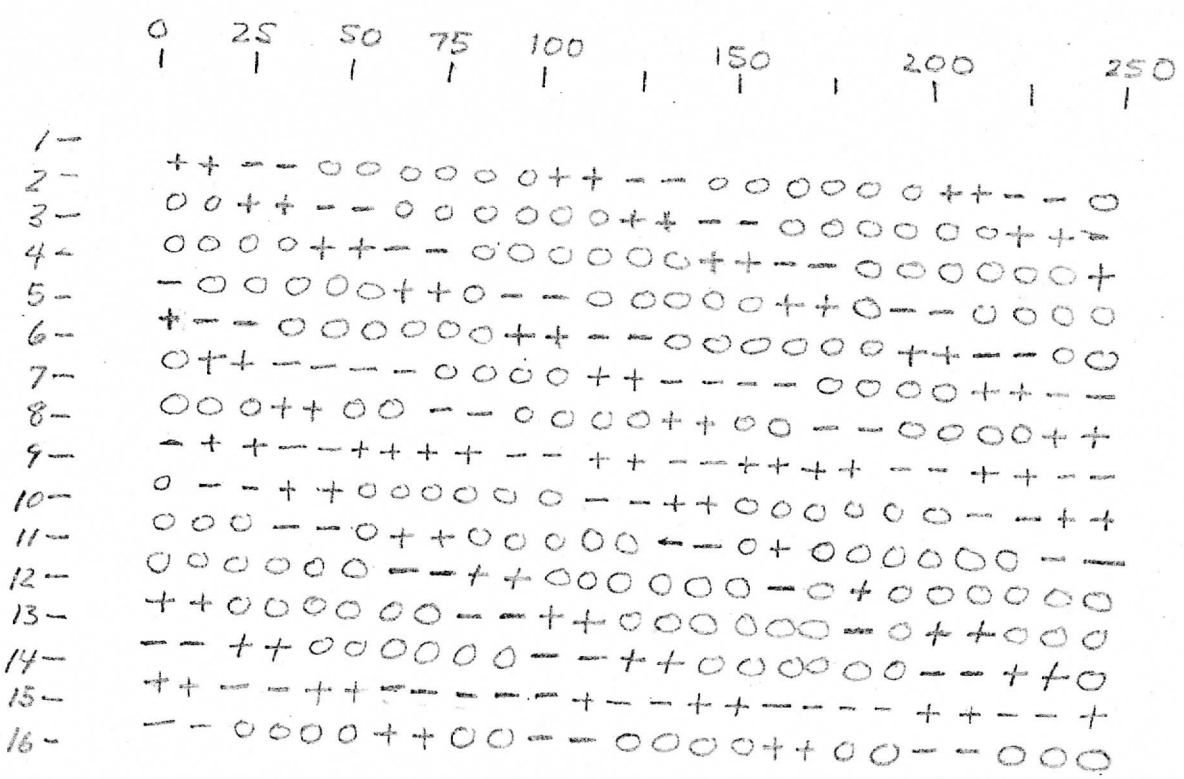

WIND SHEAR ERROR FIELD

Figure 9

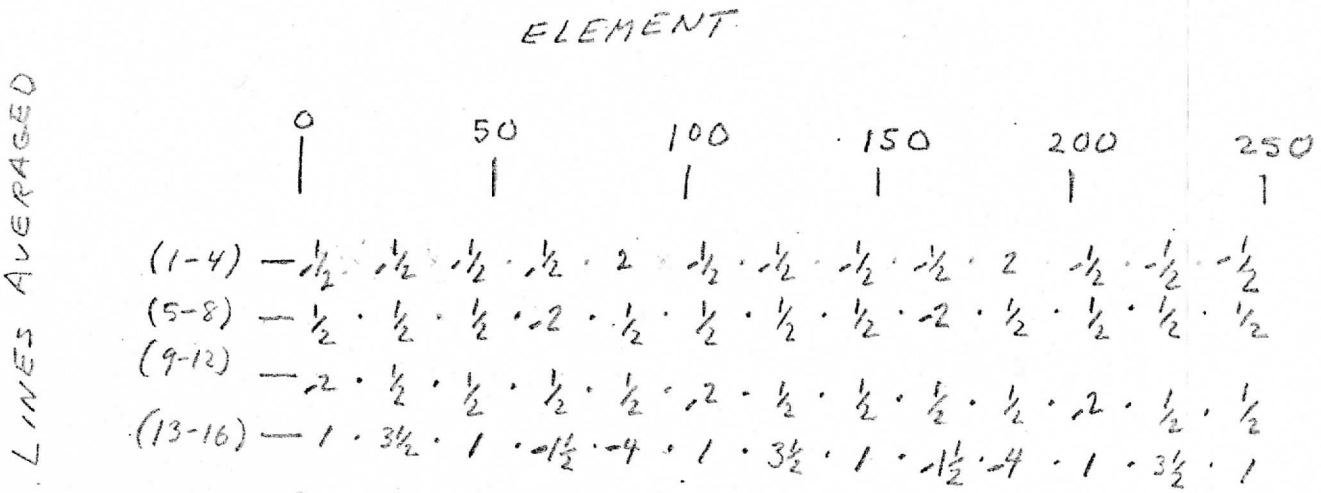

Figure 10. 1 unit = 0.10 μsec or 1 μ radiance or 0.025 n. mi.

V. POSSIBILITIES FOR IMPROVEMENTS

All calculations made in previous sections have assumed that there is no timing error introduced by the interpolation process. Since there is actually no measurement made at the midpoint of the ET sampling interval, this assumption is not strictly true. In fact, if the prealiasing filter bandpass were large compared to the original sampling frequency, the midpoint interpolated samples could often be in error by as much as $\frac{1}{2}\tau_{ET}$, resulting in an EA resampling error as large as τ_{ET}, amounting to no improvement over resampling without interpolation. The specific timing error for this case would depend on two parameters: (1) the phase between the cloud edge (e.g.) and the original sampling positions and; (2) the phase between the original sampling and the EA sampling.

In the case of the SMS VISSR, the original sampling is sufficiently frequent relative to the prealiasing bandpass to determine cloud edge locations to within 0.05 IFOV (or $\simeq$ 0.1 μsec), regardless of the phase of the sampling relative to the cloud edge. As indicated in Figure 11, which is taken from the Philco Ford Design Report C, Vol. I, Book 1, p. 2-157, this is possible because the finite detector aperture and the prealiasing filter spreads the system response to the cloud edge over several samples (the 10% to 90% rise time is near 3.0 μsec).

In principle, then, it is possible to construct interpolated samples with an RMS time jitter of 0.1 μsec within each interval between two original samples. This holds true for any number of interpolations within an interval, although nothing is gained by interpolating at intervals smaller than the 0.1 μsec jitter. It is quite clear from these considerations that midpoint interpolation will come very close to halving the EA resampling error $\frac{1}{2}\tau_{EA}$ = 1.0 μsec >> 0.1 μsec jitter). This is true even for linear interpolation of

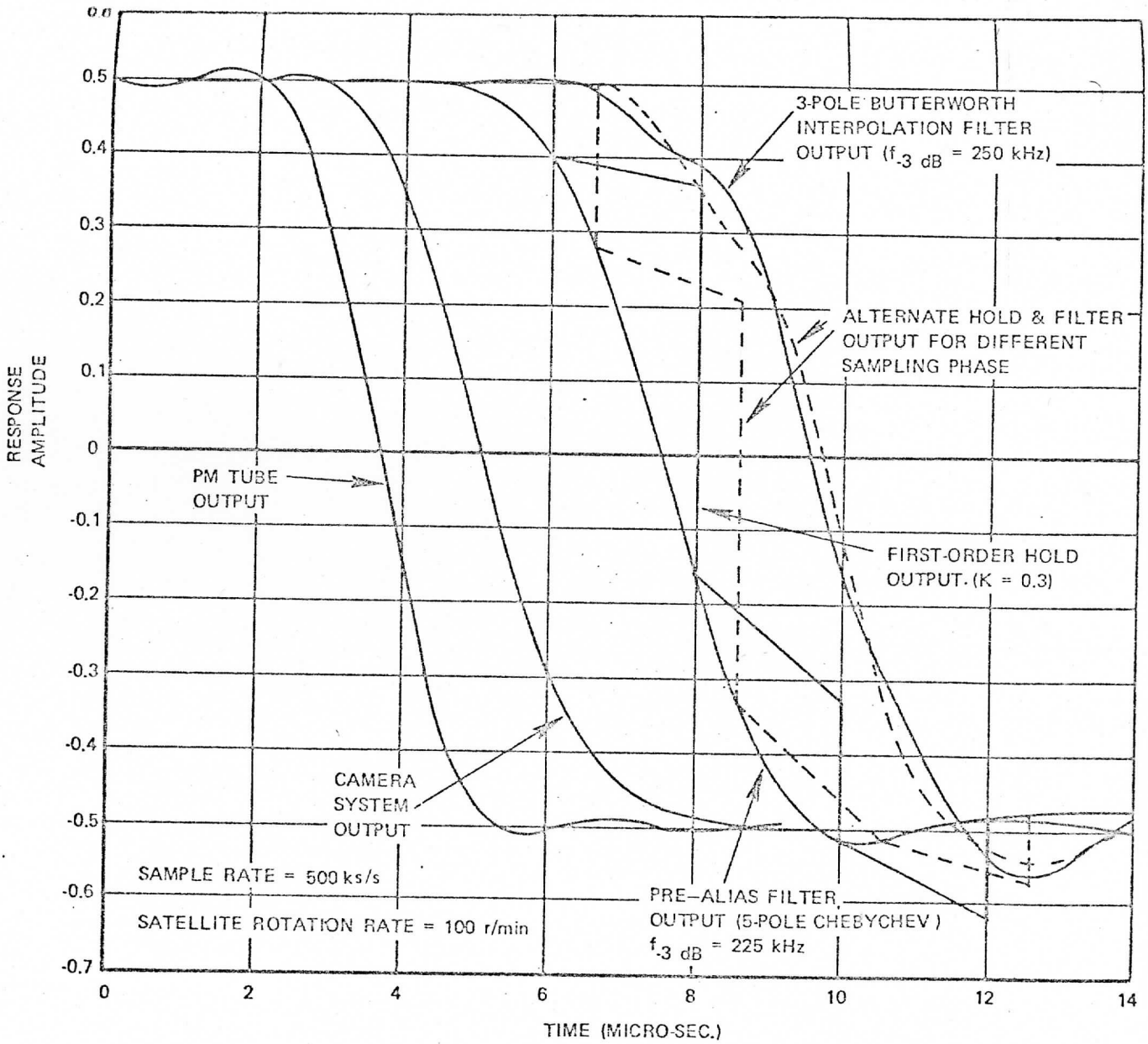

Figure 11. System Response to Image Step Function, Showing Edge Jitter Due to Sampling

the non-linearly digitized S/C signal, as demonstrated by a Westinghouse group (S/DB Design Plan, Oct. 71, p. 2-29, 2-33. Figure 12 summarizes their results for a simulated cloud edge input. They found peak to peak timing errors in the 50% point of 1.6 μsec and 0.8 μsec for the original and midpoint interpolated sets respectively, although their results are somewhat suspicious (the first error is almost certainly 2.0 μsec, not 1.6 μsec).

If three samples were interpolated between each two original samples the EA resampling error could be reduced to $\frac{1}{4}\tau_{ET} \simeq 0.5$ μsec peak to peak plus 0.1 μsec RMS jitter, neglecting the errors of linear interpolation of non-linear signals. The actual improvement could be determined easily by a computer simulation similar to that done by Westinghouse.

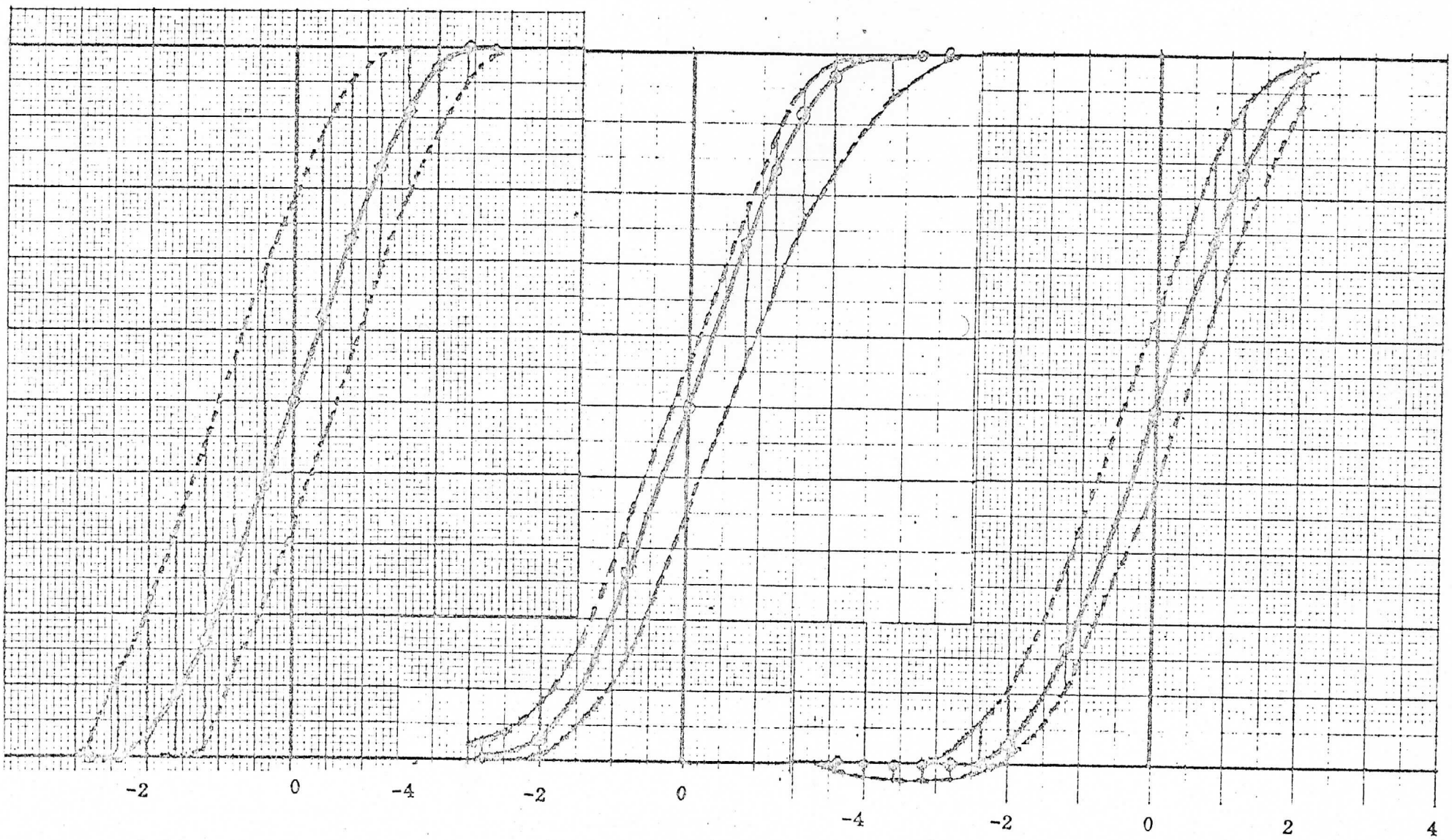

Resampled Step Waveform
- No Interpolation

Resampled Step Waveform
- Two Sample - Midpoint

Resampled Step Waveform
- Four Sample - Midpoint

Figure 12. The dashed lines indicate the bounds of the time jitter introduced by resampling.

VI. EA RESAMPLING OF IR DATA

The pointing errors introduced by resampling the IR S/C samples have the same form as that produced by resampling the visible data. However, there are two important differences:

(1) there is no line to line error correlation, i.e., the starting time is random for each IR line, and;

(2) the value of $\frac{1}{2}\tau_{ET}$ is 4.0 μsec instead of 1.0 μsec.

Thus the peak to peak timing error due to IR resampling is four (4) times that of the visible channels, although this represents a smaller fraction of the IFOV, i.e. ≃ 1/4 IFOV instead of ≃ 1/2 IFOV.

VII. SUMMARY AND RECOMMENDATIONS

1) Summary

Equal angle resampling of visible and IR S/C equal time samples produces systematic sawtooth errors in timing (or position) along a line. The phase of this sawtooth error function is random from one line to another, except in the case of visible lines within the same group of eight (8), which have fixed relative phase relationships. The resulting displacement errors of clouds moving parallel to the scan lines have a square wave form along a scan line, and introduce systematic patterns of convergence and wind shear errors. Errors for clouds which also move normal to scan lines are not so systematic and require further analysis to determine what characteristic error patterns might exist.

Several of the simplest error parameters for the SMS visible and IR resampling are summarized in Table 2. The period of the error waves is not shown since it strongly depends on spin rate (see equations (15) and (17), and Figure 3.) The effectiveness of data averaging in reducing displacement errors is not shown because of its complicated dependence on the samples averaged. (For general behavior see section IV (3).)

2) Recommendations

2.1) Construct computer simulation to assess the error pattern effects under realistic conditions: clouds moving varying amounts parallel and normal to scan lines, and clouds having a variety of sizes.

2.2) Test the effectiveness of double midpoint interpolation (3 samples between each original pair), as a means to reduce resampling timing error. It might be necessary to recommend this approach if the results of (2.1) indicate that present errors are not tolerable.

Table 2. Gross characteristics of resampling errors.

Position Error (Sawtooth Along Scan)	Peak-to-Peak	Maximum (Absolute)	RMS[1]
Visible (1/2n.mi. x 1/2n.mi.)	1.0 μsec 0.25 n.mi.[2]	0.5 μsec 0.125 n.mi.	0.29 μsec 0.007 n.mi.
IR Window (4n.mi. x 2n.mi.)	4.0 μsec 1.0 n.mi.	2.0 μsec 0.5 n.mi.	1.16 μsec 0.28 n.mi.
Displacement Error (Square Wave Along Scan)			
Clouds moving parallel to scan direction			
Visible (1/2n.mi. x 1/2n.mi.)	1.0 μsec 0.25 n.mi. 0.5 knots[3]	1.0 μsec 0.25 n.mi. 0.5 knots	0.58 μsec 0.14 n.mi. 0.28 knots
IR Window (4n.mi. x 2n.mi.)	4.0 μsec 1.0 n.mi. 4.0 knots	4.0 μsec 1.0 n.mi. 4.0 knots	2.32 μsec 0.56 n.mi. 1.12 knots

Notes 1. RMS values are obtained by averaging over all possible ET to EA starting time differences; RMS errors along a line can in general be different from these averages.

2. Errors in n. mi. are for the subsatellite point only.

3. Velocity errors are based on a frame to frame interval of 30 minutes.